第 37 卷第 3 期
2018 年 6 月

红 外 与 毫 米 波 学 报
J. Infrared Millim. Waves

Vol. 37, No. 3
June, 2018

文章编号: 1001 - 9014(2018)03 - 0275 - 04

DOI: 10.11972/j.issn.1001 - 9014.2018.03.004

Thermal analysis of electron gun for W-band gyro-traveling-wave amplifier

XU Shou-Xi[1], HOU Xiao-Wan[1], WANG Zhan-Dong[2], LIU Gao-Feng[1], GU Wei[1], GENG Zhi-Hui[1]

(1. Key Laboratory of High Power Microwave Sources and Technologies,
Institute of Electronics, Chinese Academy of Sciences, Beijing 100190, China;
2. Jinan Technician College, Ji'nan 250031, China)

Abstract: Thermal and deformation analysis of W-band gyrotron traveling wave tube amplifier (Gyro-TWTA) electron gun are carried out by using the finite element code ANSYS in the paper. Temperature distribution and thermal deformation of the cathode component at given heater power are simulated. These results are verified experimentally in an electron gun. The measured temperature distribution is in agreement with the simulation prediction. Finally, the electron trajectories with and without considering deformation are simulated by EGUN code.

Key words: thermal analysis, Gyro-TWTA, cathode component

PACS: 84.40.Ik

W 波段回旋行波管电子枪热分析

徐寿喜[1], 侯筱琬[1], 王占东[2], 刘高峰[1], 顾 伟[1], 耿志辉[1]

(1. 中国科学院电子学研究所 高功率微波源与技术重点实验室,北京 100190;
2. 济南市技师学院,山东 济南 250031)

摘要: 利用有限元软件 ANSYS 对 W 波段回旋行波管电子枪进行了热应力分析. 在给定热子功率下对阴极组件的温度场分布和热形变分布进行了模拟,并通过实验进行验证. 测试的温度分布基本与模拟结果基本一致. 最后,利用 EGUN 软件对电子枪形变前后进行了模拟.

关 键 词: 热分析; 回旋行波管; 阴极组件

中图分类号: TN129 **文献标识码:** *A*

Introduction

High-power coherent millimeter-wave sources have been extensively studied for many applications including millimeter wave radars, electronic counters measures, material process, plasma heating and high-energy particle accelerations. Based on electron cyclotron maser (ECM) mechanism, Gyro-traveling-wave tube amplifier (Gyro-TWTA) can provide significantly higher powers employing over-mode smooth waveguide [1-4]. It has numerous potential applications in many fields such as high-resolution radar and communication system [5-6].

The performance of gyrotron traveling wave tube (Gyro-TWT) greatly depends on the performance of the electron gun. A high quality electron gun with the low velocity spread is an important part of the Gyro-TWTA [7-8].

The W-band gyro-TWT use the triode type magnetron injection gun (MIG) with a modulating electrode to generate a beam of electrons. The cathode component of MIG consists of a barium-tungsten cathode and focus electrode with heat filament and support structures. The MIGs used in gyrotron devices are usually operated under temperature-limited conditions [9]. The beam current is dependent on the temperature of the cathode. In addition, when the Gyro-TWT operates, the cathode temperature can reach well in excess of 1 000℃. Due to thermal expansion, the dimensions of the cathode component at operating temperature are different than the dimensions at cold conditions. Therefore, it is necessary to take into account their thermal conductivities and expansion properties.

This paper presents the thermal and structural analysis of electron gun of a W-band gyro-TWT with the help of CAD technique.

Received date: 2017-10-09, **revised date:** 2018-01-13 **收稿日期:** 2017-10-09, **修回日期:** 2018-01-13

Foundation items: Supported by the National Natural Science Foundation of China (60971072, 61571418, 11575015 and 61531002)

Biography: Xu Shou-Xi (1971-), male, Laizhou, Shandong Province, China, Ph. D. Research fields include high power millimeter wave source and technology. E-mail: xushouxi@mail.ie.ac.cn

1 Thermal analysis

The cathode component consists of cathode emitter ring, heat filament, focus electrode, metal support shell and hold-down ring.

When the filament is powered, the heat is transferred to the cathode emitter ring. When the cathode surface temperature reaches about 1 050℃, electrons are emitted by thermionic emission. The purpose of thermal analysis is to optimize the cathode component structure of the electron gun, so that the temperature field distribution of the emitter ring is uniform, and the heating power of the filament can be reduced as much as possible in the case of the hot operation temperature.

In the thermal analysis model of magnetron injection gun, the heat transfer method is mainly based on thermal conduction and heat radiation.

The equation for heat conduction is expressed as follows [10]:

$$\frac{\partial}{\partial x}\left(k_{xx}\frac{\partial T}{\partial x}\right)+\frac{\partial}{\partial y}\left(k_{yy}\frac{\partial T}{\partial y}\right)+\frac{\partial}{\partial z}\left(k_{zz}\frac{\partial T}{\partial z}\right)+\rho Q=\rho c\frac{\partial T}{\partial t}, \quad (1)$$

where ρ is material density of electron gun, c is material specific heat, and k_x、k_y、k_z is thermal conductivity of materials in various directions, respectively. T is temperature, and Q is the thermal flow.

From the equation, the first three represents the heat transfer into the model unit. The fourth is heat generation of the model. The fifth item is the change of model temperature.

When the thermal equilibrium is reached, the transient heat conduction becomes the steady state heat balance equation. The equation is simplified as follows:

$$\frac{\partial}{\partial x}\left(k_{xx}\frac{\partial T}{\partial x}\right)+\frac{\partial}{\partial y}\left(k_{yy}\frac{\partial T}{\partial y}\right)+\frac{\partial}{\partial z}\left(k_{zz}\frac{\partial T}{\partial z}\right)+\rho Q=0. \quad (2)$$

For heat radiation, the heat flow between the two planes is directly proportional to the four square of the absolute temperature of the object surface.

$$Q_{ij}=\varepsilon\sigma A_1 F_{12}\left(T_i^4-T_j^4\right), \quad (3)$$

where T is the absolute temperature of the surface, σ is Stefen-Boltzmann constant, A1 is radiating surface area of 1, F_{12} is the shape factor of radiation surface 1 to 2, ε is the radiation rate on the surface. Obviously, the radiation is mainly depends on the material radiation rate, the surface area and the temperature difference of electron gun. In the cathode component, the heat which is from the cathode filament is transferred to the cathode surface by heat conduction, and then radiates to the surrounding.

The main parameters of our designed magnetron injection gun are given in Table 1. With the obtained geometric dimension, the model of the cathode component is constructed in ANSYS software [11]. Figure 1 shows the structural model of the cathode component of MIG for the W-band gyro-TWT.

First we choose unit type Solid70 to calculate the temperature distribution. The cathode material is mainly porous tungsten, and the focusing electrode is made of molybdenum. Both the supporting structure and hold-down ring consist of stainless steel.

Table 1 Parameters of the electron gun
表1 电子枪参数

Beam voltage	70 kV
Beam current	6 A
Cathode angle	49°
Cathode radius	11.8
current density	6.9 A/cm^2

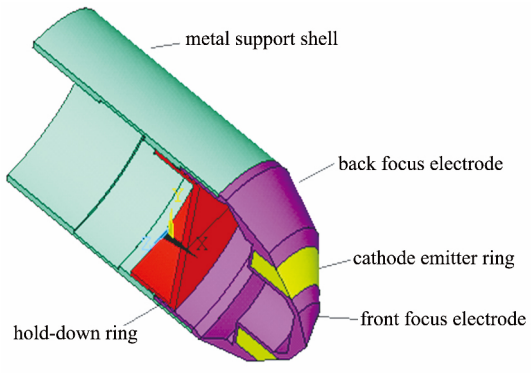

Fig. 1 The schematic view of the cathode component
图1 阴极组件结构示意图

After modeling geometry and defining material parameters(such as thermal conductivity, Young's modulus, thermal expansion coefficient) of electrodes, we add the power of 45 W to the filament by the way of heat flux and assume that the external environment temperature is 25℃. After steady analysis, we calculate the temperature distribution of the cathode component, which is given in Fig. 2. Table 2 lists the temperature range.

The temperature of the cathode emitter ring is about 1 070℃ and reaches the electron emission temperature.

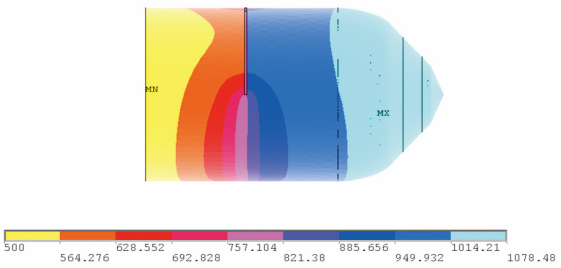

Fig. 2 Temperature distribution of the cathode component
图2 阴极组件的温度分布

Table 2 The temperature range of all the components
表2 阴极组件的温度范围

components	Temperature range/℃	
Cathode emitter ring	1 061	1 070
Front focus electrode	1 066	1 078
Back focus electrode	970	1 055
Hold-down ring	927	991
Metal support shell	500	1 020

2 Thermal deformation analysis

In order to calculate the thermal deformation of the cathode component, we use structural analysis unit SOLID185 transformed from unit SOLID70 in ANSYS software. The temperature distribution obtained above is in-

put and used as the load for thermal stress analysis. So the cathode component thermal deformation is obtained under the current temperature distribution.

Assuming that the reference temperature is 25℃, that is to say, the cathode component deformation under this temperature is zero. Then we can get the deformation of the cathode component easily. The axis deformation distribution of the cathode component is given in Fig. 3. The maximum axis thermal deformation of cathode emitter ring is 0.102 mm. Table 3 gives the axis deformation of each part of the cathode components. The calculated results show that the thermal deformation of cathode component is very small. From the simulation results, we know that the radial deformation of the cathode component is very much smaller than the axis deformation. So we can neglect the radial deformation.

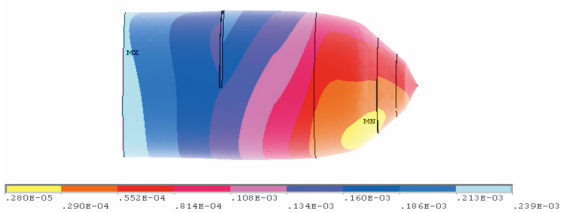

Fig. 3　The thermal deformation distribution for the cathode component

图 3　阴极组件的热形变分布

Table 3　Thermal deformation of each part of the cathode components

表 3　阴极组件的热形变

components	deformation
Cathode emitter ring	0.102 mm
Back focus electrode	0.131 mm
Front focus electrode	0.168 mm
Metal Support shell	0.239 mm
Hold-down ring	0.188 mm

According to the thermal deformation based on the aforementioned analysis, the performance of electron beam with and without deformation is calculated respectively using electronic optics EGUN software. The calculated results are shown in Table 4. The MIG structure and electron beam trajectory are obtained as shown in Fig. 4.

Table 4　The change of electron beam properties before and after deformation

表 4　形变前后电子注性能的变化

Electron beam parameter	Before deformation	After deformation
Electron voltage /kV	70	70
Electron current /A	6	6
Velocity ratio	1.03	1.04
velocity spread	1.6%	1.8%
Guide center radius / mm	0.96	0.964

From the table, we can see that the velocity ratio of the electron beam is increased by 0.01 after thermal deformation. The velocity spread is also increased by 0.2%. Calculation results show that thermal deformation of electron gun will have little impact on the performance.

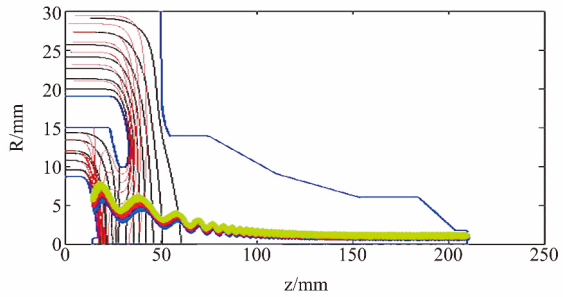

Fig. 4　Electron trajectory for the W-band MIG design

图 4　W 波段电子枪电子轨迹

3　Thermal experiment

In order to compare the results of ANSYS simulation, the temperature measurement is investigated on the cathode surface. The cathode component is placed in a vacuum environment. Vacuum is achieved with a pumping system (consisting of a mechanical pump, a turbo molecular pump and an iron pump) and a quartz glass cover is used to keep high vacuum environment. Figure 5 shows the measurement equipment.

Fig. 5　Schematic diagram of experimental setup

图 5　实验装置示意图

The voltage and current of the cathode filament are gradually increased and the vacuum is maintained at 10^{-5} Pa. To measure the steady state temperature of the cathode ring, it is necessary to stay for 10 minutes at a given heater power. The temperature is measured using optical pyrometer. The temperature distribution on the cathode emitter ring under a variety of heating power is given in Table 5.

Table 5　Temperature of the cathode ring under different heating conditions

表 5　不同加热条件下阴极的温度

filament voltage/V	filament current/A	cathode emitter ring surface temperature/℃
5.1	4.6	838
5.8	5.1	901
7.2	5.9	1023
7.9	6.3	1070
8.4	6.5	1105
8.8	6.8	1129
9.0	6.9	1145

(下转第 283 页)

Fig. 9 pictures of field target experiment (target distance: 500 m, 1 200 m)

图 9 野外目标实验图像

tion angle changes 25 times. Laser illumination intensity uniformity reaches 92.7%. In the imaging experiments, the human identify distance was up to 1.2 km. Good illumination results were obtained. The zoom illumination lens of the active imaging systems has the advantages of simple structure, uniform spot, and that spot angle can change continuously. It provides a good illumination scheme for active short wave infrared imaging system.

References

[1] Marc P Hansen, Douglas S Malchow. Overview of SWIR detectors, cameras, and applications [J]. *SPIE*, 2008, **6939**: 1-11.

[2] Borniol E De Guellec, F ,Castelein P . High-performance 640 × 512 pixel hybrid InGaAs image sensor for night vision [C]. *SPIE*, 2012, **8353**: 8353-05.

[3] Nichter J E, Martin T J, Onat B M, et al. Develop multipurpose InGaAs focal plane array visible/SWIR camera for staring and range-gated applications [C]. *SPIE*, 2007, **6572**: 65720I.

[4] Richard A. IR Imaging Optics Meet Varied Needs [J]. *Photonics Spectra*, 2012, **46**(8): .

[5] Frieden B R. Lossless conversion of a plane laser wave to a plane wave of uniform irradiance [J]. *Appl. Opt.*, 1965, **4**(11): 1400-1403.

[6] Sales R. M.. Structured microlens arrays for beam shaping [J]. *Proceedings of SPIE*. 2003, **5175**: 109-110.

[7] WANG Ying-shun, LIAN Jie, GAO Shang, WANG Xiao, SUN Zhao-zong. Illumination Uniformity of Near Infrared Illuminator [J]. *Acta Photonica Sinica*, 2013,**42**(3): 258-261.

[8] Hirai T. ,Fuse K. Kurise, K. . Development of diffractive beam homogenizer [J]. *Sei Technical Review*, 2005, **60**: 17-23.

[9] YUAN Li-bo. Light source and the optical field formed by an optical fiber [J]. *Optical Communication Technology*, 1994, **18**(1): 54-64.

[10] LI Ai-yun, WANG Xiao-ying. Study on Optical Properties of Fiber Bundle Coupling LD Output Beams [J]. *ACTA P HOTONICA SINICA*, 2007,**36**(9): 1664-1667.

[11] QI Xiao-ling, WANG Fu-juan, CAI Zhi-gang, et al. Intensity distribution of transmitted beam of multimode optical fiber [J]. *Semiconductor Optoelectronics*,2003,**24**(2): 117-120.

[12] DU Yu-nan MU Da, LIU Ying-ying, WANG Wen-sheng. Design of 20 × Long Wavelength Infrared Zoom Optical System. *Infrared Technology* [J], *Infrared Technology*, 2013,**35**(10) ,607-611.

(上接第 277 页)

As can be seen from the table, when the heating power is 49.7 W, the temperature of the cathode emitter ring is about 1 070℃, while the surface temperature simulated by ANSYS software is 1 134℃. The relative error is lower than 6% between the simulation result and experiment data.

4 Conclusion

Thermal analysis of the W-band gyrotron traveling wave electron gun is carried out by using finite element software ANSYS. The temperature distribution and thermal deformation of the cathode component are obtained when the heating power of the filament heater is 45 W. The temperature of the cathode emitter ring is about 1 070℃. The maximum thermal deformation of the cathode surface is 0.102 mm under this temperature. By using EGUN software, the performance of the electron beam with and without the deformation is not changed very much. Finally, thermal analysis results are compared with experimental values. It turns out that simulation results are consistent with experiment results.

References

[1] Barker R J,Schamilogl E. *High-Power Microwave Sources and Technologies* [M]. Piscataway, NJ: IEEE, 2001.

[2] Thumm M. , State-of-the-art of high power gyro-devices and free electron masers update 2011 KIT Scientific Reports 7606. [EB OL] http://uvka.ubka.uni-karlsruhe.de/shop/download.

[3] Chu K R. The Electron Cyclotron Maser [J]. *Rev. Modern Phys.* 2004,**76**: 489-540.

[4] McDermott D B, Song H H, Hirata Y, *et al*. Design of a W-band TE_{01} mode gyrotron traveling-wave amplifier with high power and broad-band capabilities [J]. *IEEE Trans. Plasmas Sci.*, 2002, **30**(3): 894-902.

[5] Felch K L, Danly B G, Jory H R, *et al*. Characteristics and applications of fast-wave gyrodevice [J], *Proc. IEEE*, 1999, **87**: 752-781.

[6] Nguyen K T, Calame J P, Pershing D E, *et al*. Design of a Ka-Band Gyro-TWT for Radar Applications, *IEEE Trans. Electron Devices*, 2001, **48**(1): 108-115.

[7] Lawrence R. Ives,Philipp Borchard,George Collins, *et al*. Improved Magnetron Injection Guns for Gyrotrons [J]. *IEEE Transaction on Plasma Science*, 2008, **36**(3): 620-629.

[8] Nguyen K T, Danly B G, Levuch B, *et al*. Electron gun and collector design for 94 GHz gyro-amplifiers [J]. *IEEE Trans. Plasma Science*, 1998,**26**(3): 799-813.

[9] Gilmour A S, Klystrons Jr. *Traveling Wave Tubes*, *Magnetrons*, *Crossed-Field Amplifiers*, *and Gyrotrons* [M]. Artech House, 2011: 583-626.

[10] Yang shiming, Tao wenquan, *Heat Transfer* [M],4rd, Higher Education Press, 2006.

[11] Reference Manual for ANSYS 10.0 [M], ANSYS Inc.